SLAC-PUB-4079
September 1986
(N)

WAKEFIELD ACCELERATION: CONCEPTS AND MACHINES

Perry B. Wilson

Stanford Linear Accelerator Center
Stanford, California 94305

INTRODUCTION

An introduction to the basic concepts of wake fields and wake potentials is presented in Richard K. Cooper's paper "Wake Fields: Limitations and Possibilities" in these proceedings. In this lecture we explore the possibility of using wakefield concepts to accelerate electrons and positrons to the high energies required by the next generation of linear colliders.

Brightness in Linear Colliders

In a linear collider, electron and positron bunches accelerated in opposing linacs are directed toward a collision point between the two linacs. The intensity of the collision is measured by the luminosity, defined as

$$\mathcal{L} = \frac{N^2 f_r}{4\pi \sigma_\perp^2} \,. \tag{1}$$

Here N is the number of particles in the electron and positron bunches (assumed to be equal), f_r is the bunch repetition frequency and $\sigma_\perp$ is the transverse dimension of the bunch, assumed for simplicity to be gaussian and round. We note that the units of $\mathcal{L}$ are $cm^{-2}\ sec^{-1}$. Thus the luminosity multiplied by the cross section for the occurrence of a particular event in the beam-beam collision gives the number of events produced per second. The transverse bunch dimension in Eq. (1) can be expressed in terms of the invariant emittance ϵ_n, the beam energy γ normalized to the electron rest energy, and the beta function at the beam collision point β^* as

$$\sigma_\perp = (\epsilon_n \beta^*/\gamma)^{1/2} .$$

Using this expression together with the average beam current $I_{ave} = eNf_r$ and the peak beam current $I_p = eNc/(2\pi)^{1/2}\sigma_z$ in equation (1) we obtain

$$\mathcal{L} = \frac{1}{2(2\pi)^{1/2} e^2 c} \left[\frac{I_{ave} I_p}{\epsilon_n}\right]\left[\frac{\gamma \sigma_z}{\beta^*}\right] . \tag{2}$$

The bunch length σ_z must be less than β^* in order to avoid loss of luminosity due to variation of the transverse bunch dimensions during the beam-beam collision. Furthermore, it can be shown under reasonable assumptions that

*Work supported by the Department of Energy, contract DE-AC03-76SF00515.
(Invited talk presented at the NATO Advanced Study Institute on High Brightness Accelerators, Petlachry, Scotland, July 13-25, 1986)

β^* scales with energy as $\gamma^{\frac{1}{2}}$, and that $\sigma_z \sim \lambda_{rf} \sim \gamma^{\frac{1}{2}}$ in order to keep the total ac wall plug power for a collider with reasonable bounds. Thus the last factor in Eq. (2) is roughly invariant, and the luminosity then depends only on the "brightness" $B \equiv I_{ave} I_p / \varepsilon_n$ given by the general factor.

The concept of brightness in a linear collider can be carried further by introducing the relative energy spread in the bunch $\delta \equiv \Delta E/E$. The β^* that can be achieved for a given δ varies as δ^2. Thus an extended definition of collider brightness would be $B \equiv I_{ave} I_p / \varepsilon_n \delta^2$.

Acceleration Concepts

A number of mechanisms have been proposed for the acceleration of particles to the 300 GeV - 5 TeV energy range desired for future linear colliders. (An efficient and economical single bunch acceleration scheme could also be useful as an injector into storage rings for particle physics, synchrotron radiation and FEL's.) The concepts that have been suggested range from the more-or-less conventional, such as a traditional disk-loaded accelerator structure powered by microwave tubes, to more exotic schemes, such as laser and plasma accelerators. Although the principal topic of this paper is the wakefield acceleration mechanism, it is useful to place the wakefield scheme in context by comparing it with other acceleration concepts proposed for high energy linear colliders. First, however, we will discuss some simple but basic concepts common to any acceleration method.

Figure 1 gives a conceptual diagram of an accelerator. In general an accelerator consists of some sort of driver which produces electromagnetic energy (not necessarily rf), which is converted into an accelerating field in some kind of structure. A figure of merit for the driver is the efficiency with which it converts average input ac power into the electromagnetic power delivered to the structure. A figure of merit for the structure is the effective elastance per unit length, defined as the square of the unloaded accelerating gradient divided by the input electromagnetic energy per unit length. The accelerating structure must, of course, be appropriate for each particular driver. Some proposed drivers and structure combinations are listed in Table I.

In the first three concepts in Table I, the electromagnetic energy is produced external to the accelerating structure. Concept number three is the so-called two beam accelerator. The high current external beam, running parallel to the accelerator, can be accelerated either by induction linac units or by superconducting rf cavities. Rf energy can be extracted either by an FEL interaction or by bunches interacting with longitudinal fields in a transfer cavity. In both cases the driving beam is simply an external source of rf energy. Concepts 4 through 8 involve the production of electromagnetic energy internal to the structure. Concepts 4 and 5 are the standard wakefield accelerator mechanisms in which a high-charge driving bunch is injected into an appropriate metallic structure. Electromagnetic wakefields set up behind the driving bunch can in turn be used to accelerate a trailing lower-charge bunch. Figure 2 shows the details of concept 4, in which a ring driving beam is used. In concept 5 both beams are injected on the axis of a more-or-less conventional periodic accelerating structure. Both of these wakefield schemes will be discussed in detail in the following sections. In concept 7 a driving bunch is injected into a plasma, setting up intense plasma oscillations and associated electromagnetic fields behind the bunch. This is also a wakefield acceleration method, which will be discussed briefly in a later section.

Table I

Some Driver and Structure Combinations

	Driver	Structure
A.	External Drivers	
1.	Discrete microwave tubes	Disk-loaded or other periodic metallic structures.
2.	Laser	Metallic grating or other periodic open resonator.
3.	Low energy, high current parallel external beam	Disk-loaded or other periodic metallic structure.
B.	Internal Drivers	
4.	Coaxial ring driving bunch	Radial-line wakefield transformer with annular and axial beam apertures.
5.	Collinear driving bunch	Disk-loaded or other periodic structure with axial beam aperture.
6.	Laser-switched photodiode	Radial-line transformer.
7.	Driving electron bunch	Plasma
8.	Laser	Plasma

Concept 6, sometimes called switched-power acceleration, is illustrated in Figure 3. In this method, photocathodes arranged in a ring at the outer perimeter of a radial transmission line are charged from a dc power supply. Short laser pulses trigger the photocathodes in synchronism with the accelerated beam travelling on the axis of the structure, but with an appropriate fixed time advance. The intense current emitted from the photocathode crossing the gap of the radial transmission line induces an electromagnetic pulse which travels inward toward the axis of the structure. As the radius of the ring-shaped pulse decreases, the volume occupied by the electromagnetic fields also decrease and form conservation of energy and the field strength must increase. This "transformer action" produces a large ratio between the longitudinal field strength on the axis of the structure and the field in the neighborhood of the photodiode (which in turn is approximately equal to the dc charging voltage divided by the longitudinal gap g). This transformer ratio is given approximately by[1]

$$R = 2\left[\frac{2b}{a+cT_r}\right]^{1/2} \qquad (3)$$

where τ_r is the rise time of the electromagnetic pulse, b is the radius at the photocathodes, and it is assumed that both g and $c\tau_r$ are approximately equal to the axial hole radius a. It is seen that the switched power concept is closely related to the ring-beam wakefield accelerator scheme shown in Figure 2.

(8)

Concept 8 is the laser beatwave acceleration mechanism, in which two laser beams having a frequency difference equal to the plasma frequency drive intense plasma oscillations. The fields associated with these oscillations can in turn be used to accelerate a trailing electron bunch. Only the wakefield acceleration schemes will be discussed in more detail in this paper. For a more complete description of the other acceleration mechanisms, and for the current status of analytic and experimental work in these areas, the reader is referred to Refs. 2 and 3.

Comparison of Acceleration Concepts

It is reasonable to ask what physical limitations there are for an effective figure of merit, the elastance. Suppose a uniform longitudinal accelerating field E_z is present inside a cylindrical region of radius a_{eff} and is zero outside this radius. Since magnetic fields are also necessary for propagation of electromagnetic energy, assume also that an equal amount of stored magnetic energy is present. The stored energy per unit length is then $u_{em} = \pi a_{eff}^2 \varepsilon_o E_z^2$, and the elastance per unit length is

$$s = \frac{E_z^2}{u_{em}} = \frac{1}{\pi \varepsilon_o a_{eff}^2} = \frac{3.6 \times 10^{10}}{a_{eff}^2} \quad \frac{V}{C\text{-}m} . \tag{4}$$

We see that the elastance increases inversely as the square of the energy confinement radius. As an example of the application of the concept of an effective radius for energy confinement, consider the SLAC disk-loaded structure, with an elastance of 77 V/pC-m. The effective energy radius from Eq. (4) is 2.17 cm, while the actual beam hole radius is 1.17 cm. Since energy stored outside of the beam aperture region is of no use for accelerating particles, a figure of merit for the structure is $a_{eff}/a_{geo} = 1.85$ where a_{geo} is the physical, or geometric, hole radius. From the definitions of elastance it is seen that to obtain a high value for this parameter it is only necessary to go to a structure with small transverse dimensions, for the case of an rf structure this implies for example for a short operating wavelength for an rf structure with $s \sim \lambda^{-2}$. The ratio a_{eff}/a_{geo} tells how effective the structures is with the strong dependence on physical dimensions normalized out. with similar physical dimensions are in confining electromagnetic energy near the beam axis.

In Table II some structures are compared for the various acceleration concepts that have been discussed. A rough estimate of the driver efficiency is also included. We see that the rf, wakefield and switched power acceleration schemes all have values of a_{eff}/a_{geo} in the range 1 - 2. The rf acceleration method has the advantage of high efficiency, although conventional microwave tubes with very high peak output power do not exist at very short wavelengths where the elastance is highest. The two-beam and wakefield acceleration schemes were devised basically to get around this wavelength limitation on conventional sources.

the peak power obtainable from

In concluding the discussion in this section, we note that all internal beam accelerating schemes (under B in Table I) suffer from a fundamental difficulty. The accelerated beam "sees" the wakefields of the driving beam directly, ~~both longitudinal and transverse field components.~~ In effect, the transverse deflecting fields are of the same order as the accelerating field. Thus the driving beam must be oriented with exquisite precision in the transverse direction, and in addition must be azimuthally extremely homogeneous, in order not to produce deflecting fields which are unacceptably large. In an external beam scheme, the rf is generated outside of the accelerating structure and only the accelerating component is propagated into the structure.

Table II

Comparison of Acceleration Schemes

Scheme	a_{eff}	a_{eff}/a_{geo}	a_{eff}/λ	η_D
RF (SLAC structure)	2.17 cm	1.85	0.21	0.5
Ring-beam wakefield[1)]	2.7 mm	1.34	---	0.1
Switched power[2)]	2.7 mm	$\cong$ 2	---	few %/pulse
Plasma wakefield[3)]	0.2-0.6 mm	1.0	1-2	0.1
Plasma beatwave[3)]	0.3-3 mm	3.4	3-6	< 0.1

Notes: 1) The Voss-Weiland proposal (Ref. 4).
2) Based on calculations by I. Stumer (Ref. 5). The efficiency can be improved by multiple laser pulses to the photocathodes (Ref.6).
3) Based on data in Ref. 7.

WAKE POTENTIALS IN CAVITIES AND PERIODIC STRUCTURES

Delta-Function Wake Potentials

In this section we consider wake potentials for closed cavities and periodic structures. The delta-function wake potentials for such structures are an important concept. These wake potentials are the longitudinal and transverse potentials experienced by a test charge moving at a fixed distance s behind a unit period having charge passing through the structure. The test charge is assumed to move along a path which is parallel to that of the driving charge, and both test and driving charges are assumed to move with a velocity $v \approx c$. For $v \not\approx c$ the expression for the wake potentials are in general much more complicated and the wake potential concept is less useful. The geometry of the problem is illustrated in Figure 4.

Expression for the longitudinal and transverse delta-function wake potential for the general case are introduced in Ref. 7. These potentials are simply the integrated effect of the longitudinal and transverse forms acting on a test charge as it passes through a structure (e.g. from z_1 to z_2 for the test charge T in Fig. 4) for the case of a unit point driving charge.

Under certain conditions, which will be spelled out in detail later, it can be shown[8,9] that the longitudinal and transverse wake potential can be written in terms of the properties of the normal modes of the charge-free cavity in a relatively simple way:

$$W_z(\mathbf{r}',\mathbf{r},s) = 2H(s)\sum_n k_n(\mathbf{r}',\mathbf{r})\cos\frac{\omega_n s}{c} \tag{5a}$$

$$\mathbf{W}_\perp(\mathbf{r}',\mathbf{r},s) = 2H(s)\sum_n k_{n\perp}(\mathbf{r}',\mathbf{r})\sin\frac{\omega_n s}{c} \tag{5b}$$

where

$$H(s) \equiv \begin{cases} 0 & s<0 \\ 1/2 & s=0 \\ 1 & s>0 \end{cases}$$

and

$$k_n(\mathbf{r}',\mathbf{r}) = \frac{V_n^*(\mathbf{r}')\,V_n(\mathbf{r})}{4U_n} \tag{6a}$$

$$k_{n\perp}(\mathbf{r}',\mathbf{r}) = \frac{V_n^*(\mathbf{r}')\,\nabla_\perp V_n(\mathbf{r})}{4U_n\omega_n/c} \tag{6b}$$

Here ω_n is the angular frequency the nth mode, and $V_n(r)$ is the voltage that would be gained by a nonperturbing test particle crossing the cavity in which energy U_n is stored in the nth mode. Assuming the electric field for the n^{th} mode varies with time as exp(iωt) and the position of the test particle is given by z = ct, this voltage is

$$V_n(\mathbf{r}) = \int_{z_1}^{z_2} dz\; E_z(\mathbf{r},z)\;\exp\left(\frac{i\omega_n z}{c}\right) \tag{7}$$

The conditions under which eqs. (5) are valid for the longitudinal and transverse wake functions are discussed in detail in Refs. 6 and 7, and are summarized in Table I. We see that if the driving charge and test particle

follow different paths in a closed cavity of arbitrary shape, neither Eq. (5a) nor (5b) give a valid description of the wake potentials. If the particles follow the same path in a closed cavity of arbitrary shape, Eq. (5a) is valid for the longitudinal wake potential but Eq. (5b) does not correctly describe the transverse wake potential. Formal expressions can indeed be written down for the non-valid cases, but the integrals are much more complicated, and the wake potentials for a given mode do not separate neatly into a product of an s-dependent factor and a factor which depends only on r.

Note that Eqs. (5a) and (5b) are related by

$$\frac{\partial \mathbf{W}_\perp}{\partial s} = \nabla_\perp W_z \quad . \tag{8}$$

This relation between the longitudinal and transverse wakes is sometimes termed the Panofsky-Wenzel theorem.[10] It was originally derived to calculate the transverse momentum kick received by a nonperturbing charge traversing a cavity excited in a single rf mode.

Table III

Cases for which Eqs. (5a) and (5b) give the wake potentials in the limit $v \approx c$

	Case	Eq. (5a) Valid for W_z	Eq. (5b) Valid for $\mathbf{W}_\perp$
(a)	Test charge and driving charge follow different paths in a closed cavity of arbitrary shape.	No	No
(b)	Test charge and driving charge follow the same path in cavity of arbitrary shape.	Yes	No
(c)	Velocity v is in the direction of symmetry of a right cylinder of arbitrary cross section.	Yes	Yes
(d)	Both driving charge and test charge move in the beam tube region of an infinite repeating structure of arbitrary cross section.	Yes	Yes
(e)	Both particles move near the axis of any cylindrically symmetric cavity.	Yes	Yes

The wake potential formalism, using properties of the charge-free cavity modes, makes it possible to calculate useful quantities for the charge-driven cavity. An important example is the longitudinal wake potential for the case in which the test charge and driving charge follow the same path. Equations (5a) and (6a) reduce to

$$W_z(\mathbf{r},s) = \sum_n k_n(\mathbf{r}) \cos\frac{\omega_n s}{c} \times \begin{cases} 0 & s<0 \\ 1 & s=0 \\ 2 & s>0 \end{cases} \tag{9}$$

$$k_n(\mathbf{r}) = \frac{|V_n(\mathbf{r})|^2}{4U_n} \quad .$$

The potential seen by the charge itself is

$$V(\mathbf{r},0) = -q\, W_z(\mathbf{r},0) = -q\sum_n k_n(\mathbf{r}) \tag{10a}$$

$$V_n(\mathbf{r},0) \equiv V_n(0) = -q\, k_n \quad . \tag{10b}$$

The energy left behind in the n^{th} mode after the driving charge has left the cavity is

$$U_n = -q\, V_n(0) = q^2\, k_n \quad . \tag{11}$$

The parameter k_n is the constant of proportionality between the energy lost to the nth mode and the square of the driving charge, hence the name loss parameter or loss factor.

Note from Eq. (11) that an infinitesimal distance behind a driving point charge the potential is retarding for the nth mode with magnitude

$$V_n(0^+) = 2V_n(0) = -2q\, k_n \quad . \tag{12a}$$

As a function of distance s behind the driving charge, the potential varies as

$$V_n(s) = V_n(0^+)\cos\frac{\omega_n s}{c} = -2q\, k_n \cos\frac{\omega_n s}{c} \quad . \tag{12b}$$

Equation (12a) expresses what is sometimes termed the fundamental theorem of beam loading:[11] the voltage induced in a normal mode by a point charge is exactly twice the retarding voltage seen by the charge itself.

The case of a periodically repeating structure is of obvious importance in accelerator design. Although real periodic structures are of course never infinite, practical structures at least a few periods in length seem to fulfill condition (d) of Table III. Thus the wake potentials can be computed by a summation over normal modes. For the case of a cylindrically symmetric structure, all modes depend on the azimuthal angle ϕ as $e^{im\phi}$. The wake potentials can then be written[8] for $s > 0$,

$$W_{zm} = 2\left(\frac{r'}{a}\right)^m \left(\frac{r}{a}\right)^m \cos m\phi \sum_n k_{mn}^{(a)} \cos\frac{\omega_{mn} s}{c} \tag{13a}$$

$$\mathbf{W}_{\perp m} = 2m\left(\frac{r'}{a}\right)^m \left(\frac{r}{a}\right)^{m-1} \left(\hat{r}\cos m\phi - \hat{\phi}\sin m\phi\right) \times \sum_n \frac{k_{mn}^{(a)}}{\omega_{mn} a/c} \sin\frac{\omega_{mn} s}{c} \,. \tag{13b}$$

Here $\hat{r}$ and $\hat{\phi}$ are unit vectors and $k_{mn}^{(a)}$ is the loss factor per unit length calculated at $r = a$, where a is the radius of the beam tube region. That is

$$k_n^{(a)} \equiv \frac{[E_{zn}(r=a)]^2}{4u_n}$$

where E_{zn} is the synchronous axial field component for the nth mode and u_n is the energy per unit length. The longitudinal cosine-like wake potential per period for the SLAC structure is shown in Fig. 5. Note the very rapid fall-off in the wake immediately behind the driving charge, from a peak wake of 8 V/pC per period at time $t = s/c = 0^+$. The wake seen by a point charge would be just one half of this wake, or 4 V/pC. The sine-like transverse dipole (m = 1) wake potential for the SLAC structure is shown in Fig. 6. This figure

illustrates the fact that the total wake potential is obtained by summing a finite number of modes that can be obtained using a reasonable computation time, and then adding on a so-called analytic extension to take into account the contribution from very high frequency modes. Details are discussed in Ref. 12.

Transformer Ratio for a Point Driving Charge

The transformer ratio is defined in this case as the maximum accelerating gradient anywhere behind the driving charge diodes by the retarding gradient experienced by the driving charge itself. In a single mode it is seen from Eq. (12) that for a single mode the transformer ratio R is

$$R = \frac{\text{Max } [V_n(s)]}{V_n(0)} = \frac{V_n(0^+)}{V_n(0)} = 2 \quad . \tag{13}$$

It is readily shown that this factor of two also follows directly from conservation of energy.[11] We will show later that this restriction on the transformer ratio for a point charge does not necessarily apply to an extended driving charge distribution.

A physical wake for a real cavity is a summation over many modes. Perhaps the modes might add up to produce a transformer ratio greater than two, even for a point charge. We note, however, that the wake for each mode varies with s as $W_n = 2k_n \cos(\omega_n s/c)$. At $s = 0^+$ the wakes all add in phase, and the sum of the wakes for all the modes gives a retarding potential which is exactly twice the retarding potential seen by the driving charge itself at $s = 0$. At any value of s where the net wake is accelerating, the cosine wakes for the individual modes can never do better than add exactly together in phase, as they do at $s = 0^+$. Thus

$$|W(s)| \leq \sum_n W_n(s = 0^+) = 2 \sum_n W_n(s = 0) \quad , \tag{14}$$

and the transformer ratio for a real cavity with many modes, driven by a point charge, is equal to or less than two. In practice it will be considerably less than two, since the modes will never come close to adding in phase anywhere except at $s = 0^+$. It is easy to show that Eq. (14) also follows from conservation of energy.[13]

If the driving charge and the accelerated charge follow different paths through the cavity, the situation becomes more complicated. We first note from Eqs.(5) and (6) that the longitudinal wake potential is unchanged if the paths of the driving charge and the test charge are interchanged. If we now apply conservation of energy to two charges q_1 and q_2 following different paths, we can show that

$$|W_{12}(s)| = |W_{21}(s)| \leq 2\,[W_1(0)\; W_2(0)]^{1/2} \quad , \tag{15}$$

where $W_{12}(s)$ is the wake along path 2 produced by a charge travelling on path 1, and so forth. If we define a transformer ratio R_{12} by

$$R_{12}(s) \equiv \frac{|W_{12}(s)|}{W_1(0)}$$

and similarly for R_{21}, then for any value of s

$$R_{12} \leq 2\left[\frac{W_2(0)}{W_1(0)}\right]^{1/2} = 2\left[\frac{\sum_n k_n(r_2)}{\sum_n k_n(r_1)}\right]^{1/2} \tag{16a}$$

$$R_{21} \leq 2\left[\frac{W_1(0)}{W_2(0)}\right]^{1/2} = 2\left[\frac{\sum_n k_n(r_1)}{\sum_n k_n(r_2)}\right]^{1/2} \tag{16b}$$

and

$$R_{12}\; R_{21} \leq 4 \quad . \tag{17}$$

Wake Potential in a Charge Distribution

Once the wake potential for a unit point charge is known, the potential at any point within or behind an arbitrary charge distribution with line density $\rho(s) = I(t)/c$ can be computed by

$$V(s) = -\int_s^\infty W_z\,(s'-s)\;\rho\;(s')\;ds' \tag{18a}$$

or

$$V(t) = -\int_{-\infty}^{t} W_z(t-t')\, I(t')dt'. \qquad (18b)$$

Here $W_z(\tau) = W_z(s/c)$, where τ is the time of delay after passage of the point driving charge. Similar expressions hold for the transverse potential within a charge distribution. Figure 7 shows examples of the net longitudinal potential, using the delta-function wake potential of Fig. 5 in Eq. (18a), for a gaussian bunch of unit charge in the SLAC structure. Note the reduction in amplitude of the net wake potential, over the supression of higher modes, as the bunch length increases.

Let E_a be the maximum accelerating gradient behind a driving charge distribution. It is useful to define three low parameters for the distribution as follows:

$$K_\ell \equiv \frac{E_a^2}{4\mu} \qquad (19a)$$

$$K_a \equiv \frac{E_a}{2q} \qquad (19b)$$

$$K_\mu \equiv \frac{\mu}{q^2} \quad . \qquad (19c)$$

Here μ is the total electromagnetic energy per unit length deposited by the driving charge. The three loss parameters are related by $k_a^2 = k_\ell k_y$. For a single mode k_ℓ does not depend on the charge distribution, and $k_\ell = k_n$. For a gaussian bunch interacting with a single mode, the loss parameters k_a and k_μ are given in terms of $k_\ell = k_n$ by

$$k_n(\sigma) = k_n e^{-\omega_n^2\sigma_t^2} = k_n e^{-4\pi^2\sigma_z^2/\lambda_n^2} \qquad (20a)$$

$$k_a(\sigma) = k_n e^{-\omega^2\sigma^2/2} = k_n e^{-2\pi\sigma_z^2/\lambda_n^2} \qquad (20b)$$

for each mode. Thus as the bunch length increases, coupling to higher modes is rapidly suppressed by the exponential factor. For the SLAC structure, $k_{\ell p} = 0.70/V/pC/cell$ for the fundamental mode, where p is the cell length. The amplitude of the accelerating mode voltage per cell excited by a gaussian bunch with total charge q is therefore

$$\frac{V_1}{q} = 2k_a p = 1.40\, e^{-2\pi^2\sigma^2/\lambda_0^2} \quad V/pC/cell \ .$$

For $\sigma/\lambda_0 = 0.05$, 0.20, and 0.40, this gives $V_1/q = 1.33$, 0.64 and 0.06 V/pC/cell. These values agree well with the computer calculation shown in Fig. 7.

The plot for $\sigma/\lambda_0 = 0.4$ in Fig. 7 also illustrates the phenomenon of auto-acceleration, in which fields induced by particles at the front of the bunch can accelerate particles at the tail of the same bunch.

Transformer Ratio and Efficiency for a Charge Distribution

The transformer ratio for a charge distribution is

$$R = \frac{E_a}{E_m^-} \ , \tag{21}$$

where E_a is the maximum accelerating gradient behind the bunch and E_m^- the maximum retarding gradient within the bunch. It is useful also to define an efficiency for the stransfer of energy from the bunch to the energy per unit length u is the wakefield.

$$\eta = \frac{u}{q\, E_m^-} \ . \tag{22}$$

Equations (21) and (22) can be combined with Eq. (19) to obtain

$$k_a = \frac{2\eta k_\ell}{R} \tag{23a}$$

$$q = \frac{E_a R}{4\eta k_\ell} \quad . \tag{23b}$$

WAKE POTENTIALS ON A COLLINEAR PATH WITH A CHARGE DISTRIBUTION

In the last chapter the wake potential due to a point driving charge traversing a cavity was considered under rather general conditions. We now confine our attention to the case in which the driving charge and test particle follow the same path through the cavity or structure.

For a point charge we found previously that

$$V(t) = -2q \sum_n k_n \cos \omega_n t \quad .$$

If such a charge having initial energy qV_0 is just brought to rest by the retarding wake potential at $t = 0$, then $V_0 = q \sum_n k_n$ and

$$V(t) = -\frac{2V_0 \sum_n k_n \cos \omega_n t}{\sum_n k_n} \quad . \tag{24}$$

If the structure supports only a single mode, then $V(t) = 2V_0 \cos \omega_n t$. However, a physical bunch, even a very short bunch consists of a large number of individual charges which are not rigidly connected. Thus the leading charge in such a physically real bunch will experience no deceleration, while the trailing charge will experience the full induced voltage, or twice the average retarding voltage per particle (assuming the bunch length is short compared to the wavelengths of all modes with appreciable values of k_n). The wake potential for a short charge distribution extending from $t = 0$ to $t = T$, interacting with a single mode, is illustrated in Fig. 8a. Within the bunch

the potential is given by

$$V(t) = -\frac{2V_0}{q}\int_0^t I(t')\,dt' \quad , \tag{25}$$

where V_0 is the average energy loss per particle in the distribution. This can be seen by substituting Eq. (25) in

$$V_0 = \overline{V}(t) = \frac{1}{q}\int_0^T V(t)\,I(t)\,dt \quad ,$$

and working out the double integral. Note from Eq. (25) that for t = T at the end of the distribution V(T) = $-2V_0$. Therefore $V_m^+ = 2V_0$, $V_m^- = |-2V_0| = 2V_0$ and the transformer ratio is $R = V_m^+/V_m^- = 1$.

The potential in and behind a long charge distribution is shown schematically in Fig. 8b. We consider first the case for a single mode. From Eq. (18b) with $W_z(t) = 2k_n \cos \omega_n t$,

$$V_n(t) = -2k_n\int_{-\infty}^t I(t')\cos\omega_n(t-t')\,dt' \quad . \tag{26}$$

Assume now that the bunch extends in time from -T to +T. Within the bunch (-T < t < T) the retarding potential is

$$V_n^-(t) = -2k_n\left[\cos\omega_n t\int_{-T}^t I(t')\cos\omega_n t'\,dt' + \sin\omega_n t\int_{-T}^t I(t')\sin\omega_n t'\,dt'\right] . \tag{27}$$

Following the bunch (t > T) the accelerating potential is

$$V_n^+(t) = 2k_n\left[\cos\omega_n t\int_{-T}^T I(t')\cos\omega_n t'\,dt' + \sin\omega_n t\int_{-T}^T I(t')\sin\omega_n t'\,dt'\right] . \tag{28}$$

If the bunch is symmetric about t = 0, the second integral in Eq. (28) vanishes, and $V^+(t)$ reaches a maximum value given by

$$V_m^+ = 2k_n \int_{-T}^{T} I(t') \cos\omega_n t' \, dt' \quad . \tag{29}$$

The retarding potential at the center of such a symmetric bunch is given by

$$V^-(0) = -2k_n \int_{-T}^{0} I(t') \cos\omega_n t' \, dt' = -\frac{1}{2} V_m^+ \quad . \tag{30}$$

If $V^-(0)$ happens also to be the maximum (absolute) value of the retarding potential, then $|V^-(0)| = V_m^-$, and the transformer ratio is $R = V_m^+/V_m^- = 2$. If $V^-(0)$ is not a the peak of the retarding potential, then $V_m^- > |V^-(0)|$ and $R < 2$. Thus for symmetric bunches interacting with a single mode, the transformer ratio cannot exceed two. This upper limit is reached only if the maximum retarding potential is reached at the center of symmetry of the distribution. Otherwise, the transformer ratio is less than two. If the bunch is not symmetric, the preceeding argument does not apply. The transformer ratio can then in principle be arbitrarily large, as we will see shortly.

The limitation $R \leq 2$ tends to apply for symmetric bunches even in the case of a physical structure with many modes. For example, in Fig. 7, showing gaussian bunches in the SLAC structure, the transformer ratios for $\sigma/\lambda_o = 0.05$, 0.20, and 0.40 are seen to be 1.4, 1.9 and 1.4 respectively. It is possible in principle to imagine a structure in which several modes cooperate to produce $R > 2$ for symmetric bunches.[14] However it is not probable that the limitation $R = 2$ can be exceeded by a significant amount in any physically realizable structure.

Symmetric Driving Bunches

Let us now turn to the case of an asymmetric driving bunch. Take as an example a triangular current ramp in a single mode cavity. Let $I(t) = I\omega t$ for $0 < t < T$ and $I(t) = 0$ otherwise. For simplicity let the bunch length be $T = 2\pi N/\omega$, where N is an integer. Then within the bunch

$$V^-(t) = 2kI\omega \int_0^t t' \cos\omega(t-t')\, dt' = -\frac{2kI}{\omega}\,(1-\cos\omega t) \quad , \tag{31a}$$

whereas behind the bunch

$$V^+(t) = 2kI\omega \int_0^T t' \cos\omega(t-t')\, dt' = 2kIT\, \sin\omega t \quad . \tag{31b}$$

Thus $V_m^- = 4kI/\omega$, $V_m^+ = 2kIT = 4\pi kIN/\omega$ and

$$R = \frac{V_m^+}{V_m^-} = \pi N \qquad \left\{\begin{matrix}\text{current ramp,}\\ \text{single mode}\end{matrix}\right\} \quad . \tag{32}$$

The wake potential for a current ramp of length N = 2 interacting with a single mode are shown in Fig. 9a.

In a real structure with many modes, one might expect that the transformer ratio will be less than that given by Eq. 32. The potential excited in the SLAC structure by a current ramp with N = 2 is shown in Fig. 10. Within the bunch the retarding potential has a behavior close to the single mode calculation, $V^-(t) \sim 1 - \cos\omega t$. However, some energy goes into higher modes, as is evident by ripples on the cosine wave behind the bunch. This causes a degradation of the transformer ratio from the single mode prediction $R = 2\pi$ to $R = 4.86$. The degradation worsens as the bunch gets longer, as can be seen in Fig. 11.

The efficiency for energy extraction from a driving bunch extending from $t = 0$ to $t = T$ in which all of the electrons have the same energy $eV_0 = eV_m^-$ is

$$\eta = -\frac{1}{qV_m^-}\int_0^T I(t)\, V^-(t)\, dt \quad . \tag{33}$$

For a linear current ramp interacting with a single mode, substitution of Eq. (31a) together with appropriate expressions for $I(t)$, V_m^- and q into Eq. (33) gives an efficiency of 0.5 if $\omega T = 2\pi N$. A higher efficiency and a higher transformer ratio could be obtained if the retarding potential could be made as flat as possible across the current distribution. In the limit $V^-(t) = V_m^- = \text{constant}$, Eq. (33) gives an efficiency of 100%. In Ref. 14 it is proven that the potential can be exactly flat only for a current distribution which consists of a delta function followed by a linear current ramp, where the proper relation exists between the value of the delta function and the slope of the current ramp. In this limit the transformer ratio is given by[14]

$$R = \left[1 + (2\pi N)^2\right]^{1/2} \qquad \left\{\begin{array}{c}\text{Delta function plus}\\ \text{current ramp,}\\ \text{single mode}\end{array}\right\} \quad . \tag{34}$$

Here $N = \omega T/2\pi = cT/\lambda$, and N can now take non-integer values. For large N the transformer ratio approaches $R \approx 2\pi N$ and the efficiency approaches 100%. The transformer ratio for the delta function alone ($N \to 0$) is $R = 1$, as we know is the case for all short bunches, and the efficiency is 0.5. An approximation to this distribution, in which the wake potential is driving negative by an exponentially decaying spike and then held constant by a rising current ramp, is illustrated in Fig. 9c.

A third distribution of interest is a linear current ramp preceeded by a quarter wavelength rectangular pulse. The response to this distribution is shown in Fig. 9b. The transformer ratio in the case of this "doorstep" distribution is[14]

$$R = \left[1 + \left(1 - \frac{\pi}{2} + 2\pi N\right)^2\right]^{1/2} \qquad \left\{\begin{array}{c}\text{Doorstep plus}\\ \text{current ramp,}\\ \text{single mode}\end{array}\right\} . \tag{35}$$

In the limit of large N transformer ratio again approaches $R \approx 2\pi N$. For long bunches the transformer ratio and the efficiency are again approximately twice that for the linear current ramp alone. Except for particles in the first quarter wavelength of the bunch, all particles experience the same retarding potential. At the end of the doorstep (N = 1/4), R = $\sqrt{2}$ and $\eta = 2/\pi$.

As a numerical example, consider an accelerator operating at λ = 1 cm with a desired gradient of 200 mV/m. A SLAC-type structure at this wavelength would have a loss parameter on the order 2×10^{15} V/C-m. With a transformer ratio of 20, driving bunches with an energy of 100 MeV would need to be injected every ten meters. The charge per bunch as given by Eq. (23b) is

$$q = \frac{E_a R}{4k\eta} \approx 0.5\ \mu C ,$$

assuming that most of the energy goes into a single mode and that the efficiency is close to 100%. The bunch length is approximately $R\lambda/2\pi$ = 3.2 cm or 100 ps, and the peak current at the end of the bunch is 10 kA. Many practical questions must be addressed, such as the feasibility of creating properly shaped bunches with very high peak currents. The deflecting fields induced if the driving bunch wanders off the axis of the structure are also a serious problem.

The Plasma Wakefield Accelerator

The plasma wakefield accelerator is another type of collinear acceleration scheme in which the metallic rf structure is replaced by a plasma medium. If the plasma is cold, one expects that only a single mode, the oscillation at the plasma frequency, will be excited. Thus a plasma is in essence a single mode structure in which the axis of symmetry is defined by the driving beam.

Figure 12 shows the result of a simulation[15] in which a triangular bunch one wavelength long is injected into a plasma. The transformer ratio as measured from the figure is $R \approx \pi$, in agreement with the theoretical prediction for a triangular bunch given by Eq.( ).

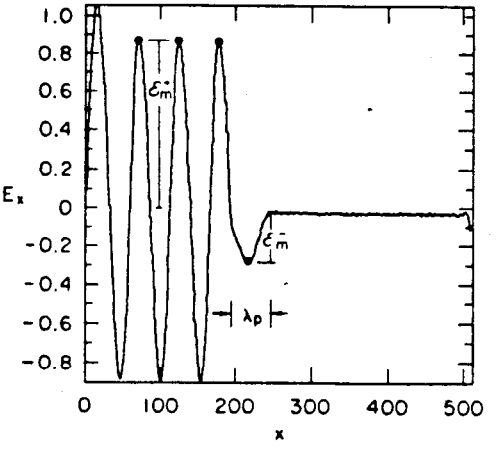

Figure 12: Wakefield of a triangular bunch in a plasma.

RING BEAMS

Transformer Ratio For A Ring Beam

Consider first a circular bunch of radius a passing between two parallel metallic planes spaced apart by a distance $g \ll a$. The energy deposited between the two plates, initially contained in a volume $V_1 \approx \pi a^2 g$,

will at some later time t be distributed over a spreading ring-shaped region of radius $b = ct$, thickness $\sim 2a$ and volume $V_2 \sim (2\pi b)(2a)g = 4\pi abg$. Thus the ratio of field strengths will be

$$R_1 \sim \left(\frac{V_1}{V_2}\right)^{\frac{1}{2}} = \left(\frac{a}{4b}\right)^{\frac{1}{2}} .$$

This also gives the approximate transformer ratio at transverse distance b from a single bunch passing between the two plates. The transformer ratio for a ring-shaped beam of radius b can now be obtained by considering that the ring is made up of $n = A_2/A_1 = 4b/a$ beamlets, giving for the net transformer ratio $R = n\, R_1 = 2(b/a)^{\frac{1}{2}}$:

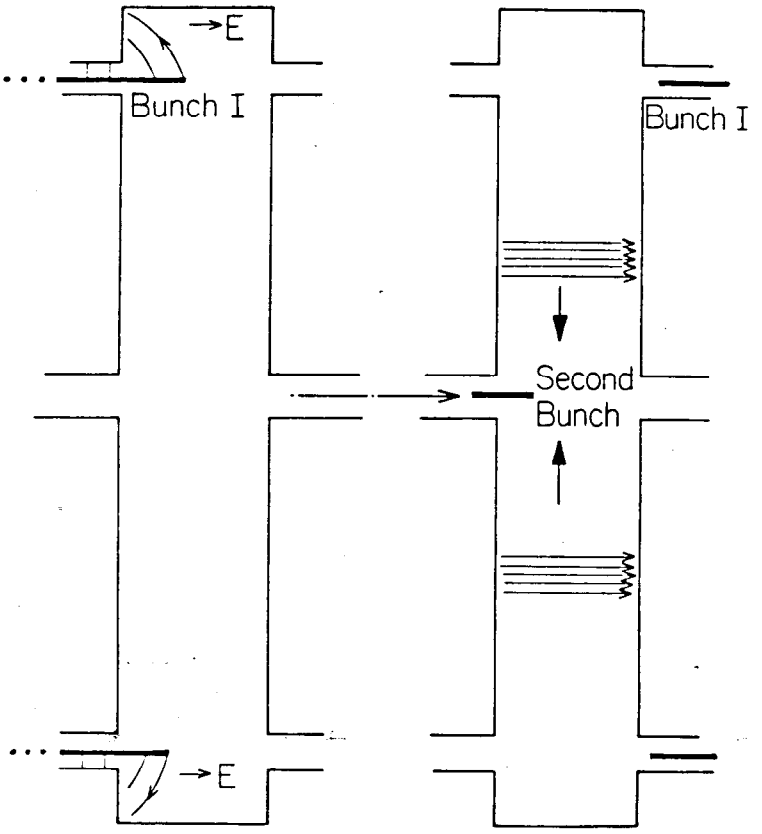

Figure 14: Qualitative picture of the field induced by a ring bunch passing through a pillbox cavity.

If now an outer cylindrical wall is added, as shown in Fig. 14, the energy that would propagate outward away from the axis is directed toward the axis, this increase R by a factor of $\sqrt{2}$, giving

$$R = 2\left(\frac{2b}{a}\right)^{\frac{1}{2}} . \tag{36}$$

This transformation is in agreement with that given by Eq. (3), introduced earlier for the switched radial transmission line, under the assumption $a\pi g$.

The Wakefield Transformer

The wakefield transformer, illustrated in Fig. 2, consists essentially of a series of pillbox cavities, of the type shown in Fig. 14, having a ring gap near the outer radius for the driving beam and a hole on the axis for the accelerated beam. A wakefield transformer of this type was originally proposed by Voss and Weiland.[16] In reference 4 the transformer ratio is computed for a wakefield transformer of this kind with a = 2mm, b = 26 mm and g = 1.5 mm, using a particle tracking code. The peak energy gain on the axis is calculated to be 20 times the average energy loss in the ring driving bunch. However, the energy gain on the axis divided by the peak energy loss in the driving bunch (our definition of transformer ratio) is about 12. Putting the transformer dimensions into Eq. (18) we obtain R = 10, in substantial agreement with the results from the tracking code.

An experiment is underway at DESY (Deutsches Elektronen Synchrotron in Hamburg) to test this type of crucial wakefield transformer principle as a means to obtain high accelerating gradients for future linear colliders. The eventual goal is a collider in the 1 TeV energy range operating at a gradient on the order of 200 MV/m. In the prototype experiment presently in progress, a ring-shaped bunch with a charge of 1 μC will be injected at 8 MeV into a wakefield transformer to accelerate a second bunch from 8 MeV

to over 50 MeV at a gradient of 100 MV/m or greater. Details of the experiment, and the current status, are given in Refs. 3, 4 and 17.

PROTON WAKEFIELD ACCELERATION AND TEST FACILITIES

In the last section it was noted that the transformer ratio $\overline{R}$, defined as the (unloaded) energy gain in the accelerated bunch divided by the average energy loss in the driving bunch, is typically larger than the transformer ratio R based on the peak energy loss in the driving bunch. For relativistic electrons the ratio R would normally apply, since a driving bunch of electrons injected with uniform energy would deteriorate rapidly once electrons in the region of peak decelerating fields have been brought to rest. For non-relativistic particles (few hundred MeV protons) the situation is different. The particles can move back and forth within the bunch, with the lead particles and trailing particles continuously changing places. By this process of "mixing", it is possible for all of the particles to experience the average decelerating gradient. This is the basis for the proton wakefield accelerator (WAKEATRON) proposed by A. Ruggiero.[18]

For a gaussian bunch interacting with a single mode with loss parameter k_o, it was shown previously that the accelerating gradient behind the bunch is

$$E_a = 2 Q k_o e^{-\omega^2\sigma_t^2/2}$$

the average loss, on the other hand, was shown to be

$$\overline{E^-} = a/Q = Q k_o e^{-\omega^2\sigma_t^2} .$$

Therefore

$$\bar{R} \equiv \frac{E_a}{\bar{E}} = 2\, e^{\omega^2\sigma_t^2/2} \quad . \tag{37}$$

For a gaussian or very symmetric bunch it was shown that the transformer ratio $R \equiv E_a/\bar{E}_m \leq 2$, while from Eq. (13) we see that the transformer ratio $\bar{R}$ based on the average energy loss in the driving bunch, can in principle, increase without limit. On the other hand, the charge required in the driving bunch must also increase as $\bar{R}$ increases:

$$Q = \frac{E_a}{2k_o}\, e^{\omega^2\sigma_t^2/2} = \frac{E_a\,\bar{R}}{4k_o} \quad . \tag{38}$$

A facility (Advanced Accelerator Test Facility[19]) has just been completed at Argonne National Laboratory to test some of the wakefield acceleration techniques that have been described here. A 22 MeV electron linac can produce driving bunches of $1 - 2 \times 10^{11}$ electrons with pulse lengths of 5 - 150 ps and an emittance of 7 π-mm-mr. A second bunch (witness beam) can be injected to probe the longitudinal and transverse wake potentials in the range 0 - 2.4 ns behind the driving bunch. Initial experiments to test the WAKEATRON and plasma wakefield accelerator techniques are currently in the planning stage, and tests of other new acceleration concepts have been proposed for the future.

REFERENCES

1. F. Villa, SLAC-PUB-3875, Stanford Linear Accelerator Center, Stanford, California.

2. C. Joshi and T. Kastsouleas, eds. Laser Acceleration of Particles, AIP Conference Proceedings No. 130 (American Institute of Physics, New York, 1985).

3. Symposium on Advanced Accelerator Concepts, Madison, Wisconsisn, August 21-27, 1986. To be published in American Institute of Physics Conference Proceedings.

4. See articles by the Wakefield Accelerator Study Group and by T. Weiland and F. Willeke in Proceedings of the 12th International Conference on High Energy Accelerators, (Fermi National Accelerator Laboratory, Batavia, Illinois, August 1983). pp. 454-459.

5. I. Stumer, private communication.

6. Pisin Chen, to be published in the Proceedings of the 1986 Linear Accelerator Conference, Stanford, California, June 2-6, 1986. Also available as SLAC-PUB-3970.

7. Richard K. Cooper, "Wake-Fields: Limitations and Possibilities". These Proceedings.

8. K. L. F. Bane, P. B. Wilson and T. Weiland in Physics of High Energy Particle Accelerators, BNL/SUNY Summer School, 1983, M. Month, P. Dahl and M. Dienes, eds., AIP Conference Proceedings No. 127. (American Institute of Physics, New York, 1985), pp. 875-928. Also available as SLAC-PUB-3528, December, 1984.

9. K. Bane, CERN/ISR-TH/8-47, 1980.

10. W. K. H. Panofsky and W. A. Wenzel, Rev. Sci. Inst. 27, 967 (1956).

11. P. B. Wilson in Physics of High Energy Particle Accelerators, Fermilab Summer School, 1981, R. A. Carrigan, F. R. Huson, M. Month, eds., AIP Conference Proceedings No. 87 (American Institute of Physics, New York, 1982), Sec. 6.1. Also available as SLAC-PUB-2884, February 1982.

12. K. Bane and P. B. Wilson, Proceedings of the 11th International Conference on High-Energy Accelerators, CERN, July 1980 (Birkhäuser Verlag, Basel, 1980), p. 592.

13. P. B. Wilson in Proceedings of the Thirteenth SLAC Summer Institute on Particle Physics, SLAC Report No. 296 (Stanford Linear Accelerator Center, Stanford, California), pp. 273-295. Also available as SLAC-PUB-3891, February, 1986.

14. K.L.F. Bane, Pisin Chen and P. B. Wilson, IEEE Trans. Nucl. Sci. NS-32, No. 5, 3524 (1985). Also available as SLAC-PUB-3662.

REFERENCES (cont'd)

15. P. Chen, J. J. Su, J. M. Dawson, P. B. Wilson and K. L. Bane, UCLA Report No. PPG-851, 1985.

16. G. Voss and T. Weiland, DESY Report 82-074 (1982).

17. T. Weiland, IEEE Trans. Nucl. Sci. NS-32, 3471 (1985).

18. A. G. Ruggiero, Argonne National Laboratory Report ANL-HEP-CP-86-51 (1986).

19. J. Simpson et al., IEEE Trans. Nucl. Sci. NS-32, 3492 (1985).

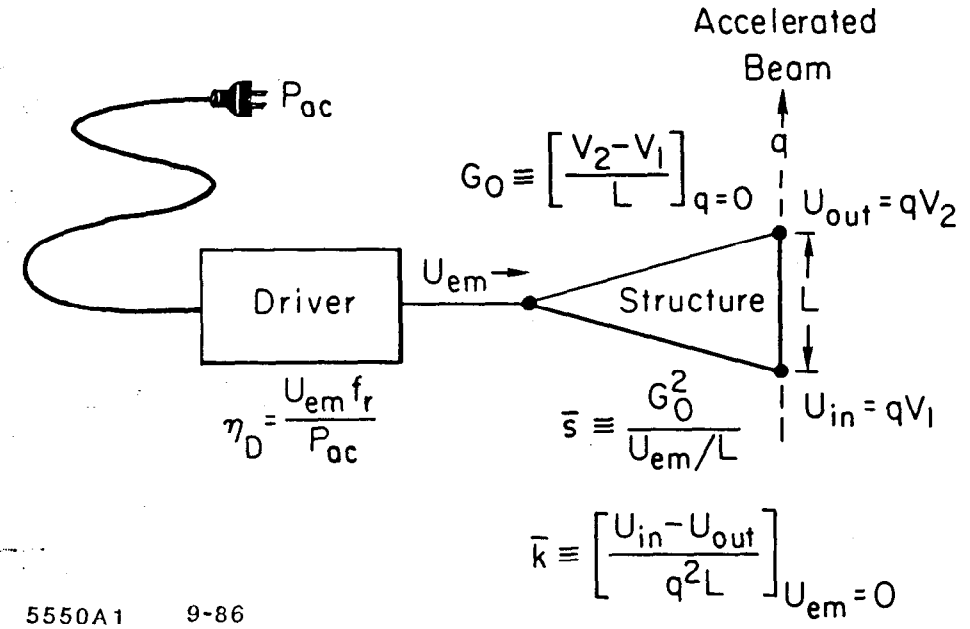

Figure 1: Conceptual diagram of an Accelerator.

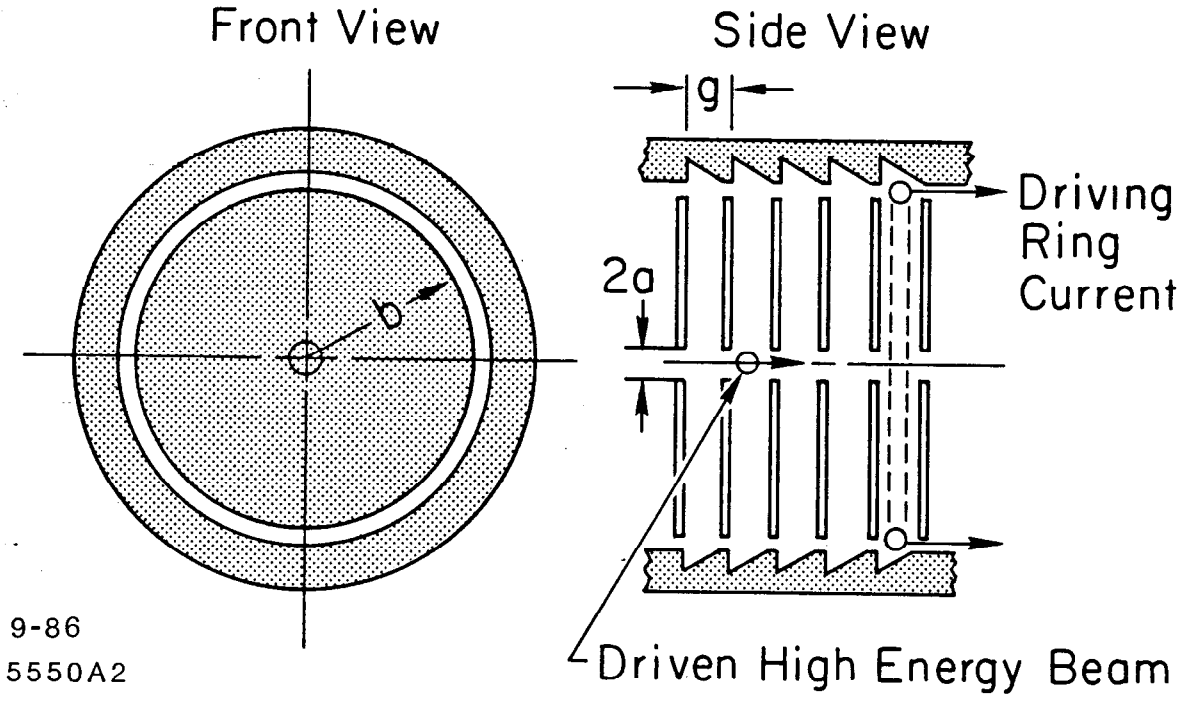

Figure 2: Wakefield Accelerator with a Ring Driving Beam.

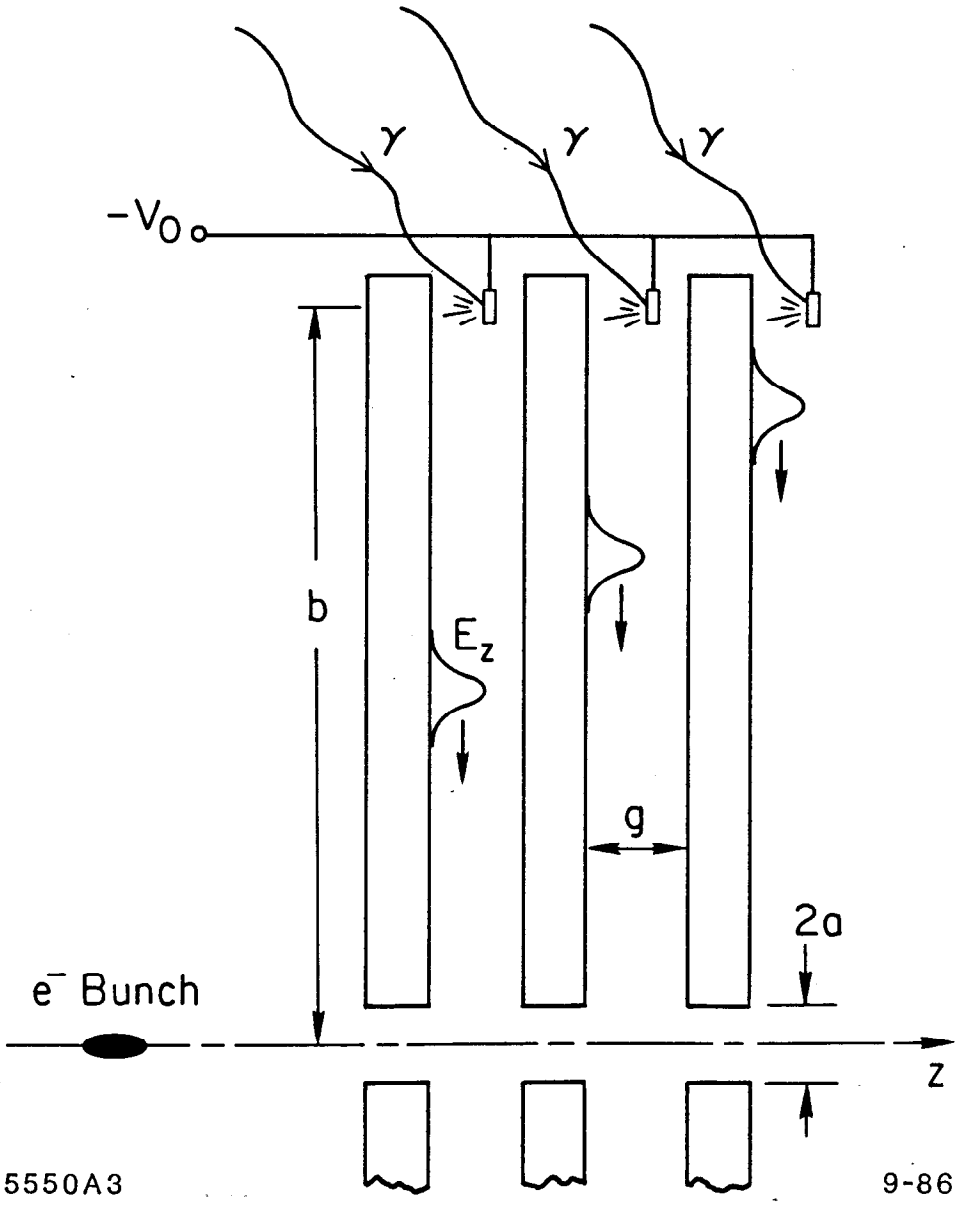

Figure 3: Switched Power Accelerator Concept.

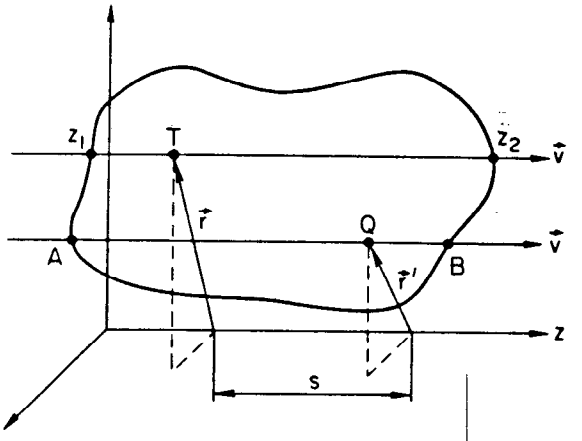

Figure 4: A driving charge Q, moving at constant velocity V parallel to the z-axis, enters a closed cavity at A(r',z=0) at t=0 and leaves at B(r',z=L). A non-perturbing test particle T also moves at the same velocity v, but at transverse position r and at longitudinal distance s behind Q.

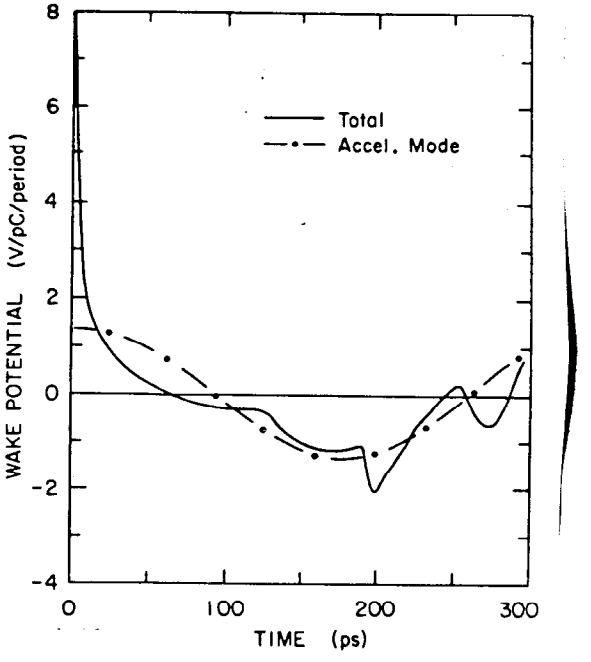

Figure 5: A longitudinal delta-function wake potential per cell for the SLAC disk-loaded accelerator structure at time t=s/c behind a point driving charge.

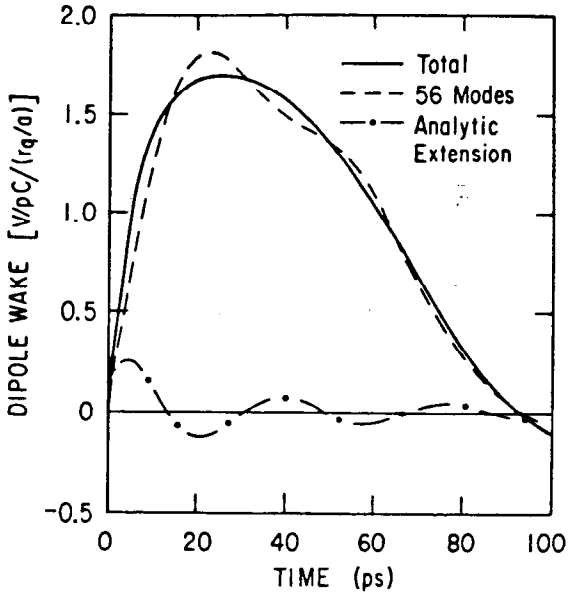

Figure 6: Dipole delta-function wake potential per cell for the SLAC structure.

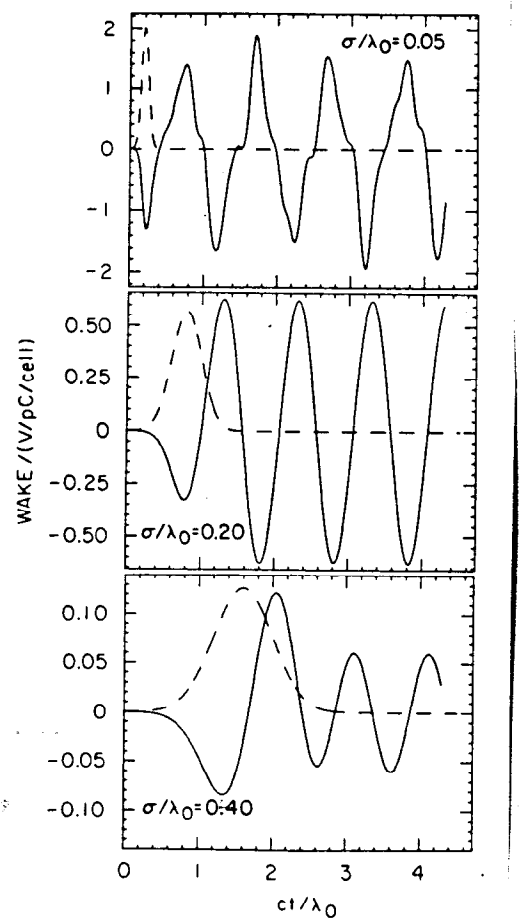

Figure 7: Potential in and behind a gaussian bunch interacting with the longitudinal modes of the SLAC structure.

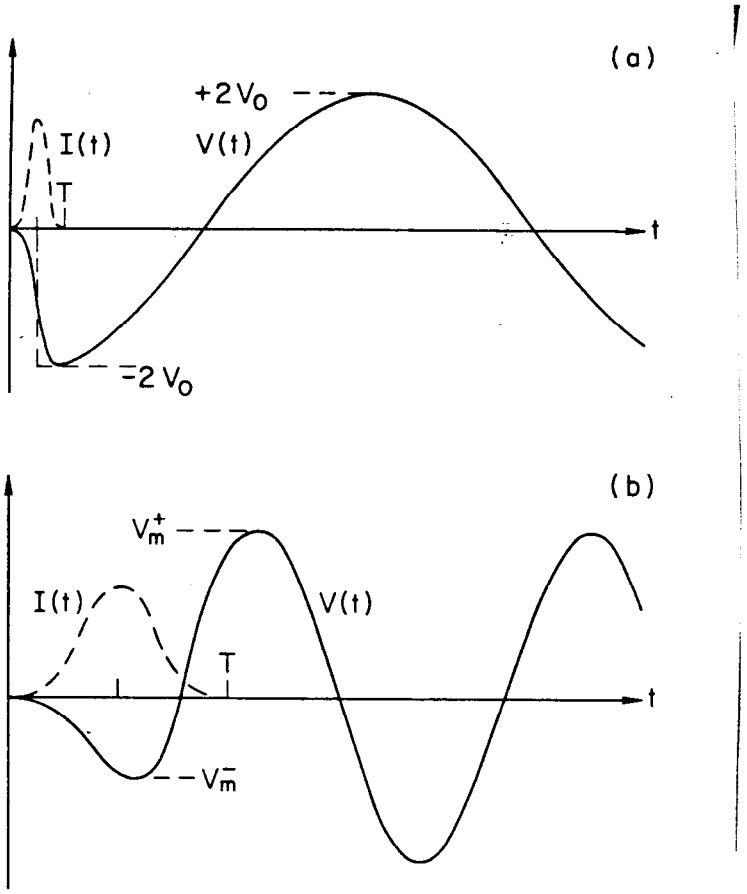

Figure 8: Potential in and behind a charge distribution interacting with a single mode for (a) a short bunch, and (b) a long bunch.

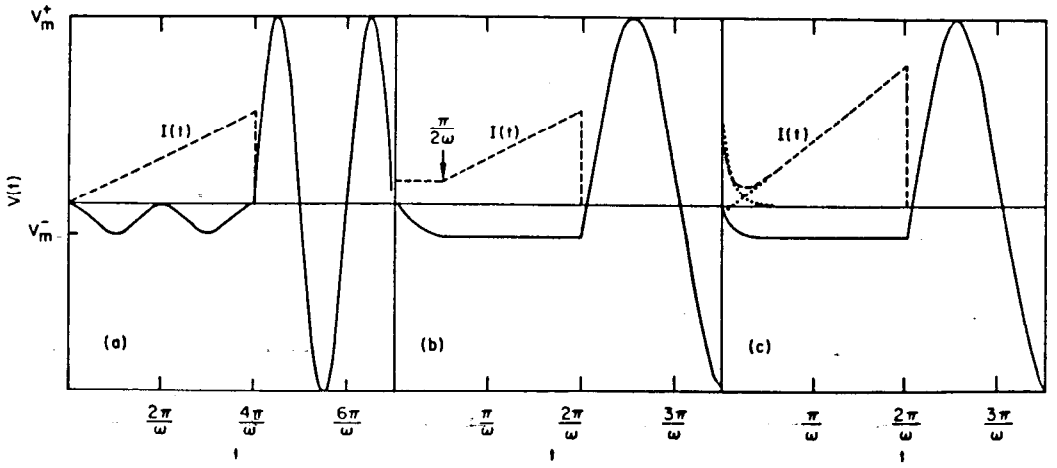

Figure 9: The voltage induced by three different asymmetric current distributions interacting with a single mode.

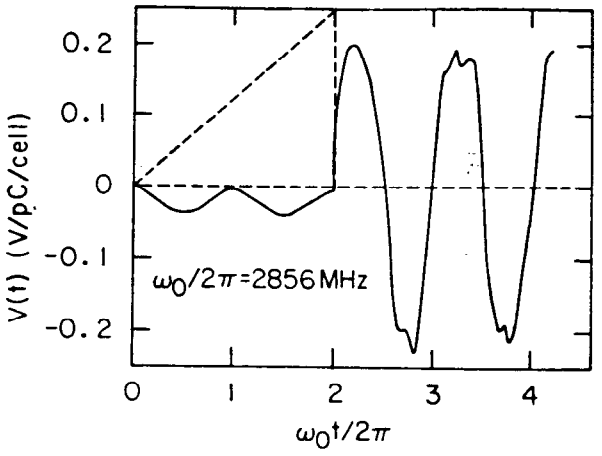

Figure 10: The potential induced by a linear current ramp interacting with the modes in the SLAC structure.

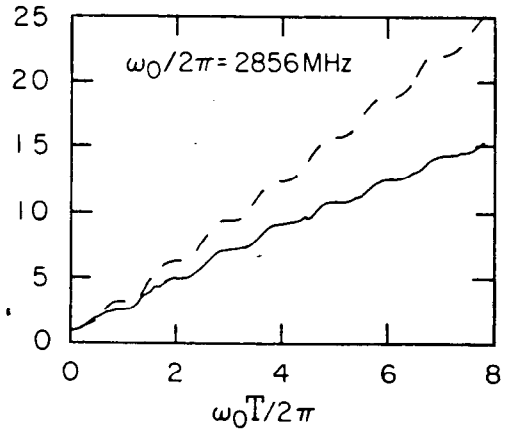

Figure 11: The transformer ratio for a linear current ramp in the SLAC structure as a function of bunch length. The dashed line gives single mode results.